

Solvent-Free Synthesis of a new Perfluorinated MIL-53(Al) with a genuine Temperature-induced breathing effect

Diletta Morelli Venturi, Virginia Guiotto, Roberto D'Amato, Lucia Calucci, Matteo Signorile, Marco Taddei, Valentina Crocellà and Ferdinando Costantino

Table of content

-Materials and methods

-structure refinement

-Adsorption/desorption volumetric measurement

-SS-NMR spectra

-FT-IR Spectra

-DSC analysis

Materials and Methods

All chemicals are commercially available and used as received from the specified vendors without further purification. Aluminum nitrate nonahydrate ($\text{Al}(\text{NO}_3)_3 \cdot 9\text{H}_2\text{O}$) was purchased from Honeywell Fluka™, tetrafluoro terephthalic acid ($\text{H}_2\text{-F}_4\text{BDC}$) was purchased from SiKÉMIA and acetone was purchased from Merck.

Powder X-ray diffraction (PXRD) patterns were collected in reflection geometry in the $4\text{-}65^\circ$ 2θ range, with a 30 s step^{-1} counting time and with a step size of 0.016° , for the phase identification after the synthesis, and in the $4\text{-}120^\circ$ 2θ range, with a 120 s step^{-1} counting time and with a step size of 0.016° , for solving the structure, on a PANalytical X'PERTPRO diffractometer, PW 3050 goniometer, equipped with an X'Celerator detector and using a Cu-K α radiation source. The long fine focus (LFF) ceramic tube operated at 40 kV and 40 mA. The sample for structure solving was treated in a muffle oven at 280°C for one hour; the heating rate used to reach the target temperature was $15^\circ\text{C}/\text{min}$.

Variable temperature Powder X-ray diffraction (VT-PXRD) patterns were recorded in air in the $25\text{-}240^\circ\text{C}$ range with an Anton Paar HTK 1200N hot chamber mounted on a Panalytical XPERT PRO diffractometer (Cu-K α radiation, $40\text{ kV} \times 40\text{ mA}$), equipped with the PIX-CEL solid-state fast detector. The scanning range was $2\theta = 4\text{-}40^\circ$ with an 8 s step counting time and 0.03° increments of 2θ . The temperature variation rate was $10^\circ\text{C}/\text{min}$; the sample was kept 5 min at the target temperature before collecting the data.

Thermogravimetric analysis was performed using a Netzsch STA490C thermoanalyzer under a 20 mL min^{-1} air flux with a heating rate of $10^\circ\text{C min}^{-1}$.

Emission Spectroscopy (ICP-OES) analysis was carried out using a Varian 700-ES series instrument. A calibration curve was obtained with four standard aluminum solutions ($0.5, 1, 2.5, 5\text{ mg L}^{-1}$ respectively). The sample for the ICP-OES measurement was prepared dissolving 2.8 mg of $\text{F}_4\text{-MIL-53(Al)}$ in 2 mL of concentrated nitric acid (c.a. 63% wt.) and then diluted in a 50 mL graduated flask with DI water.

SS-NMR experiments were carried out on a Bruker Avance Neo spectrometer working at Larmor frequencies of $500.13, 470.59, 130.32,$ and 125.77 MHz for $^1\text{H}, ^{19}\text{F}, ^{27}\text{Al},$ and ^{13}C nuclei, respectively, equipped with a double-resonance CP/MAS probe head accommodating rotors with external diameter of 4 mm . ^1H and ^{19}F spectra were recorded by Direct Excitation (DE) under magic angle spinning (MAS) conditions, accumulating 16 scans with a recycle delay between consecutive transients of 2 s . The $^{19}\text{F}\text{-}^{13}\text{C}$ cross-polarization (CP) experiment was performed under MAS conditions using a contact time of 1 ms and a recycle delay of 2 s ; 1200 scans were accumulated. The ^{27}Al DE-MAS spectrum was acquired using an excitation pulse with a duration of $0.2\text{ }\mu\text{s}$ and accumulating 1200 scans with a recycle delay of 1 s . All spectra were recorded at room temperature at a MAS frequency of 15 kHz using air as spinning gas. The chemical shift of all nuclei was referenced to the ^{13}C signal of adamantane at 38.46 ppm . ^{27}Al spectral line shape was analyzed using the Bruker software TopSpin.

Field Emission Scanning Electron Microscopy (FESEM) was performed with a FE-SEM TESCAN S9000G (TESCAN ORSAY HOLDING, Brno, Czechia) equipped with a Schottky type FEG source. The detector was an In-Beam Secondary Electron (SE) detector.

Differential Scanning Calorimetry (DSC) was performed on a Setaram Calvet C80 microcalorimeter. The sample was weighed (52.4 mg) and inserted in a cylindrical Hastelloy cell. An equal empty cell was used as reference. The heat-cool sequence was performed between 100°C and 275°C and repeated twice with a heating rate of $0.3^\circ\text{C}/\text{min}$. The lower temperature value (100°C) was set to avoid any signal related to the removal of physisorbed water. For the HeatFlow calculation, a linear baseline has been used.

IR spectroscopy was performed using a Bruker Vertex 70 spectrophotometer within the 4000-600 cm^{-1} spectral range, equipped with a MCT (mercury cadmium tellurium) cryogenic detector. The resolution of the reported IR spectra was 2.0 cm^{-1} and an average of 32 scans was used to reduce the signal to noise ratio. Before the analysis the sample, in form of self-supported pellets mechanically protected by a gold envelope, were inserted in a special home-made quartz cell with KBr windows. The cell was connected to a conventional high-vacuum glass line, equipped with mechanical and turbo molecular pumps (residual pressure $p < 10^{-4}$ mbar), that allows *in situ* adsorption/desorption measurements.

Adsorption/desorption volumetric measurement was carried out at 87 K, using Ar as probe. The isotherm was collected with a Micromeritics 3Flex sorption analyzer. About 30 mg of sample was weighed and activated at 150 °C for 30 min. Specific Surface Area (SSA) was determined by employing the Brunauer–Emmett–Teller (BET) method and following the Rouquerol consistency criteria (BET range for SSA: 0.0035 – 0.1 p/p_0).

Synthesis of F₄-MIL-53(Al)

In a Teflon seal reactor, 10 mmol of $\text{Al}(\text{NO}_3)_3 \cdot 9\text{H}_2\text{O}$ (3.75 g) and 10 mmol of $\text{H}_2\text{-F}_4\text{BDC}$ (2.38 g) were mixed together with a spatula and heated in a static oven at 120 °C for 24 hours. The mixture was washed two times in water (20 mL) for 15 minutes, once in acetone (20 mL) for 15 min and then let in acetone (20 mL) for 16 hours. The recovered product was dried overnight in static oven at 80 °C. Yield: 1.95g, 82%. The phase identity and purity were checked through PXRD.

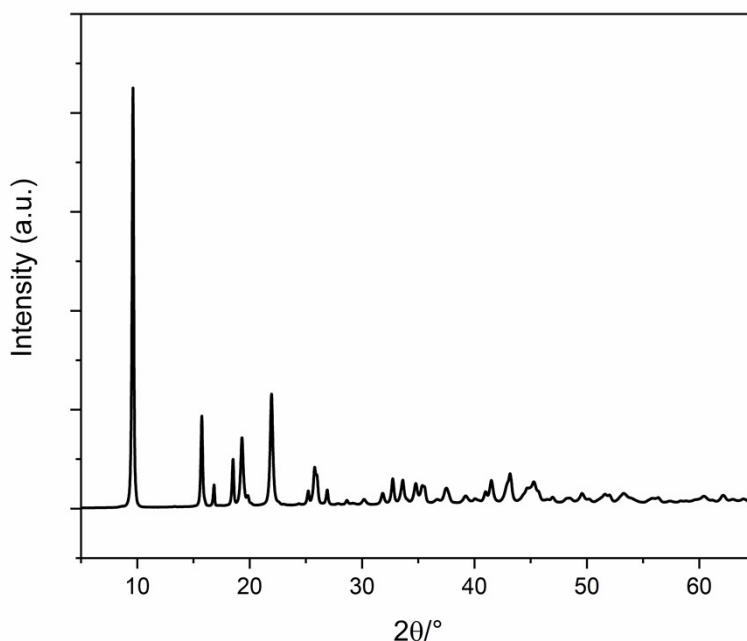


Figure S1. PXRD pattern of F₄-MIL-53(Al)

Structural refinement

Indexing of the diffraction patterns of F₄-MIL-53(Al) was performed with *TOPAS* (v. 4.2).¹ The analysis of systematic extinctions for space group assignment was performed using the *CheKcell* program.² Structure solution was performed *ab initio* using the software *FOX*.³

Initially, [AlO] atoms were employed to identify the location of the inorganic building unit. Then, the positions of one Al atom and one O atom were fixed on special positions (0.25, 0.25, 0.25) and (0, 0.25, z), respectively. Half of a F₄BDC fragment was included in the asymmetric unit. Bond lengths and bond angles were restrained to correctly reproduce the geometry of the linker. A H atom, used as a dummy, was placed on special position with coordinates (0.5, 0.5, 0.5) and restrained to sit in the middle of the aromatic ring. A set of anti-bump restraints was employed to prevent unrealistically short intermolecular contacts: Al-F = 3.0 Å; Al-C = 2.5 Å; O-F = 2.0 Å; C-C = 1.3 Å; O-O = 2.0 Å. The initial model was then refined using the Rietveld method in *TOPAS* (v. 4.2).¹ First, a Pawley refinement was carried out to model background, sample displacement, profile shape parameters (Full_Axial_Model, CS_L, CS_G) and lattice parameters (Orthorhombic). Then, Rietveld refinement was performed to model the atomic coordinates and atomic S3 displacement parameters. In order to maintain the mass center of the linker in special position (*i.e.* rotation of the aromatic ring outside of the plane defined by carboxylic groups), the aromatic ring, defined by C2, C13, C4, C11, C12, F9, F13 atoms was modelled by employing ten bond, ten angle restraints and one restraint for the dihedral angle. In order to describe the geometry of the aromatic ring correctly, a dummy atom (X1, whose occupancy factor was set to zero) was employed: X1 was placed on a special position (0.5, 0.5, 0.5), in between C4 and C11 and in the middle of the aromatic ring. The occupancies of C4 and C11 were restrained in order for their sum to be equal to one. C2 and C4 were placed on special position, respectively, (0, y, -y) and (0, y, -y). Atomic displacement parameters for all the atoms were restrained at the same value and refined together. At the end of the refinement, all the parameters were refined together until convergence. To better model the intensity of some reflections, spherical harmonics (order 6) were introduced in the refinement. Despite a clear anisotropy morphology is not shown in FESEM pictures, the tendency to form crystals with elongated shape in MIL-53 is known in literature.⁴ Due to this particular shape MIL-53 crystals may be affected by preferential orientation of basal planes that justify the use of spherical harmonics correction in the refinement.⁴ All the refinement parameters are shown in Table S1.

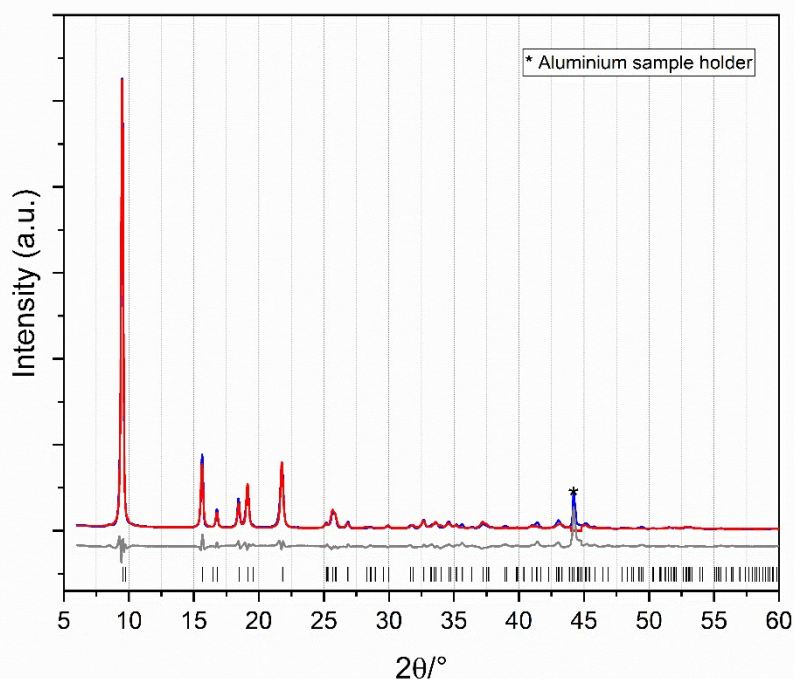


Figure S2. Rietveld refinement carried out on the PXRD pattern ($\lambda = 1.5401 \text{ \AA}$) of **F₄-MIL-53(Al)**. The experimental PXRD pattern is shown in blue, the calculated in red and the difference (experimental - calculated) is given in grey. The allowed reflection positions are given in black.

Table S1. Rietveld refinement parameters of F₄-MIL-53(Al)

| | |
|---|---|
| Formula | Al(OH)(C ₈ F ₄ O ₄) |
| M [g mol⁻¹] | 279.06 |
| Wavelength [Å] | 1.54056 |
| T [°C] | 25 |
| Crystal system | Orthorhombic |
| Space group | <i>Imma</i> |
| Z | 4 |
| a [Å] | 6.6327(16) |
| b [Å] | 18.113(5) |
| c [Å] | 10.751(3) |
| V [Å³] | 1292.1(8) |
| D_{calc} [g cm⁻³] | 1.5508(21) |
| R_p | 11.996206 |
| R_{wp} | 17.9499718 |
| R_{F2} | 4.33299045 |
| GoF | 11.9271676 |

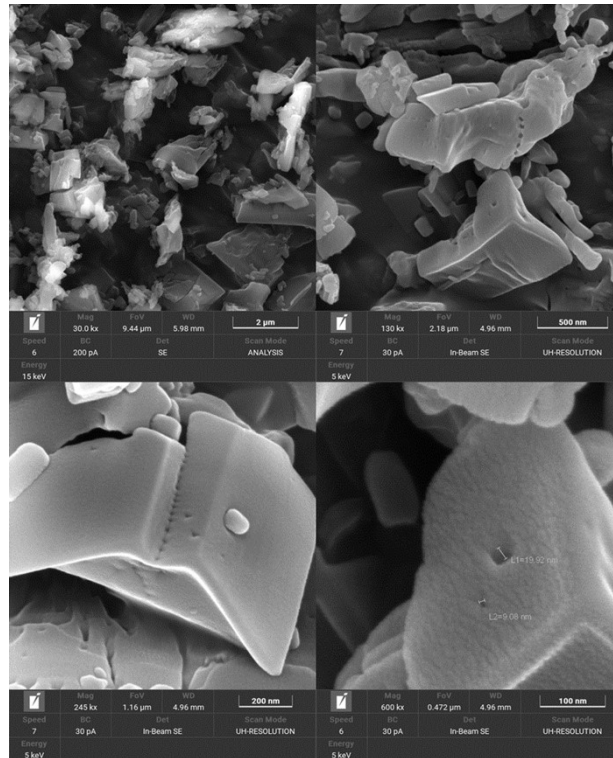


Figure S3. Fe-SEM images of F₄-MIL-53(Al).

Adsorption/desorption volumetric measurement

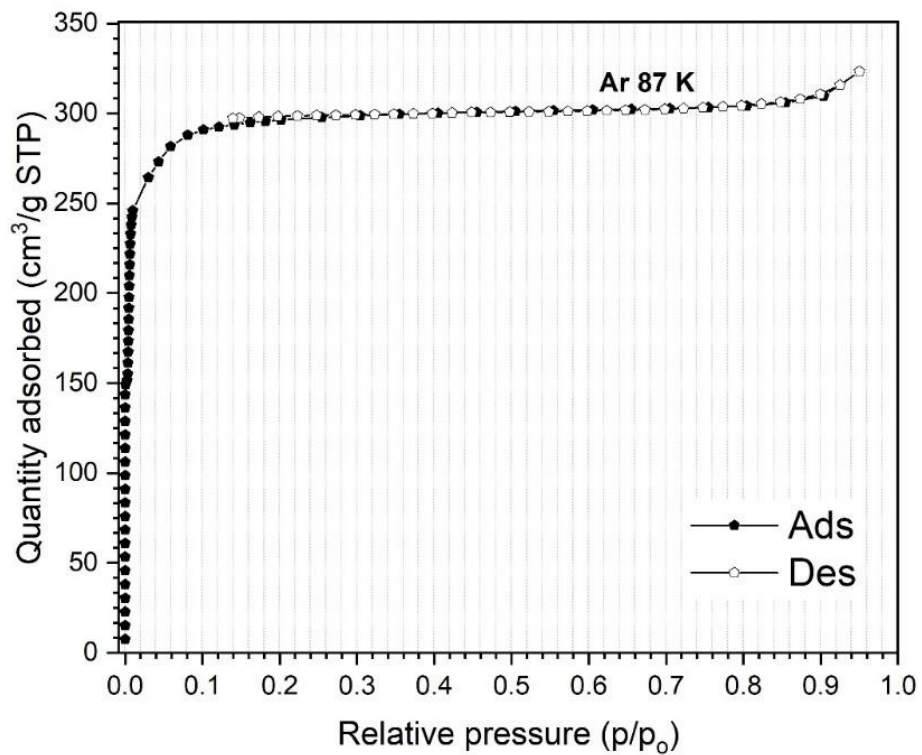


Figure S4 Adsorption/desorption isotherms of Ar adsorbed on F₄-MIL-53(Al) at 87 K. Full symbols: adsorption. Empty symbols: desorption.

SS-NMR

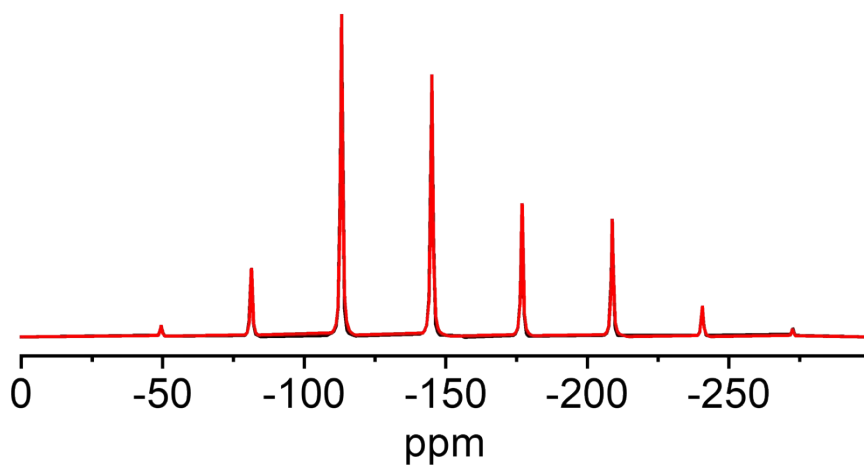


Figure S5. Experimental (black) and calculated (red) ^{19}F DE-MAS spectrum of $\text{F}_4\text{-MIL-53(Al)}$. In the spectrum calculation a chemical shift anisotropy (CSA) tensor with components $\delta_{11} = -80.9$ ppm, $\delta_{22} = -113.3$ ppm, $\delta_{33} = -240.9$ ppm was used.

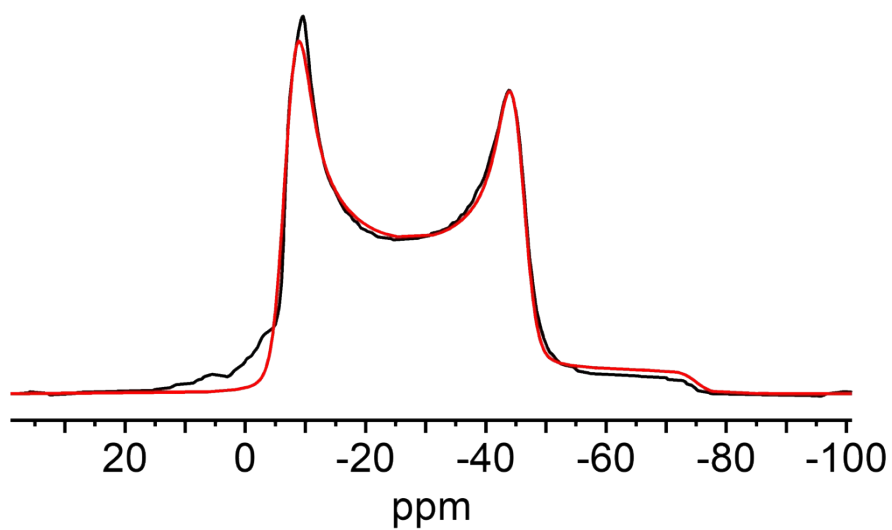


Figure S6. Experimental (black) and calculated (red) ^{27}Al DE-MAS spectrum of $\text{F}_4\text{-MIL-53(Al)}$. From the line shape analysis, the following best fitting parameters were obtained: $\delta = 3.9$ ppm, $C_Q = 9.46$ MHz, $\eta_Q = 0.0$.

Thermogravimetric analysis

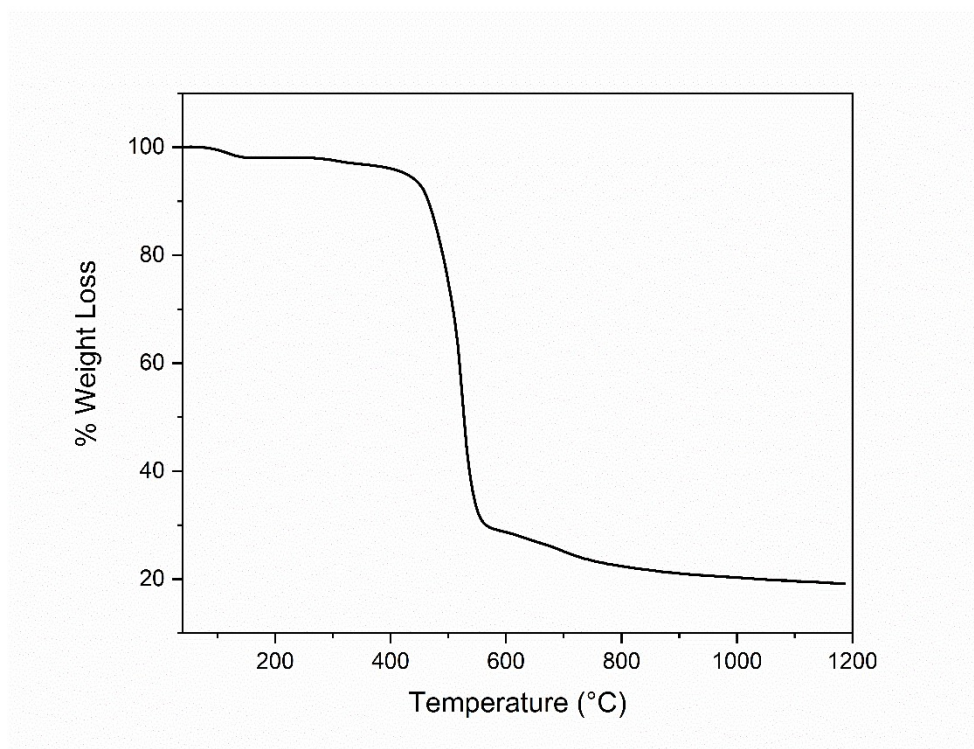


Figure S7. Thermogravimetric curve of F₄-MIL-53(Al).

IR Spectroscopy

A self-supported pellet of F₄-MIL-53(Al) was prepared and inserted in the IR cell equipped with KBr windows. The cell was introduced inside the chamber of the spectrophotometer and the first spectrum was collected (black curve in **Figure S8**). The cell was then connected to a vacuum line and sequential spectra were acquired during room temperature (RT) degassing (pale orange sequence in **Figure S8**). After 60 minutes the final spectrum of the totally outgassed F₄-MIL-53(Al) was collected (red curve in **Figure S8**). The spectra collected in the mid-IR region exhibit very intense signals (often out of scale) below 1800 cm⁻¹, as for example the asymmetric and symmetric OCO⁻ stretching vibrational modes of carboxylate moiety ($\nu_{\text{OCO}}(\text{as})$ and $\nu_{\text{OCO}}(\text{sym})$ respectively) located in the region between 1700-1400 cm⁻¹. In contrast, the spectral region at high frequency is poor of signals and can be exploited to detect the presence of possible physisorbed molecules.

The IR profile of F₄-MIL-53(Al) shows an isolated and sharp peak centered at 3692 cm⁻¹ corresponding to the stretching mode of the OH group bridging two Al atoms. The frequency of this signal matches with that of the structural OH-bridging groups of the non-fluorinated MIL-53(Al).⁵ The presence of a small fraction of water inside the MOF framework (interacting *via* hydrogen bonding with the structural OH groups) is suggested by the weak and broad component between 3600 and 2700 cm⁻¹, with apparent maximum at around 3455 cm⁻¹.^{6,7} Compared to MIL-53(Al), the broad band generated by the presence of water is definitely less pronounced and completely disappear by simply outgassing the sample at room temperature. This testifies the high hydrophobic character of F₄-MIL-53(Al) due probably to the presence of the fluorine atoms on the benzene ring.

MIL-53 is a flexible MOF which undergoes a phase transition and consequently a change in the pore dimensions upon desorption of pre-adsorbed molecules (like water). IR can be a powerful technique to detect the transition, the lattice vibrational modes being sensitive to the pore dimensions.⁸ For instance, it has been reported by many authors that the ν_{18a} mode associated to the terephthalate moieties is the most sensitive

to the pore opening. Unfortunately, this signal (located at around $1020 - 1015 \text{ cm}^{-1}$) is totally out-of-scale in the spectrum of $F_4\text{-MIL-53(Al)}$ and such information is, therefore, completely lost.

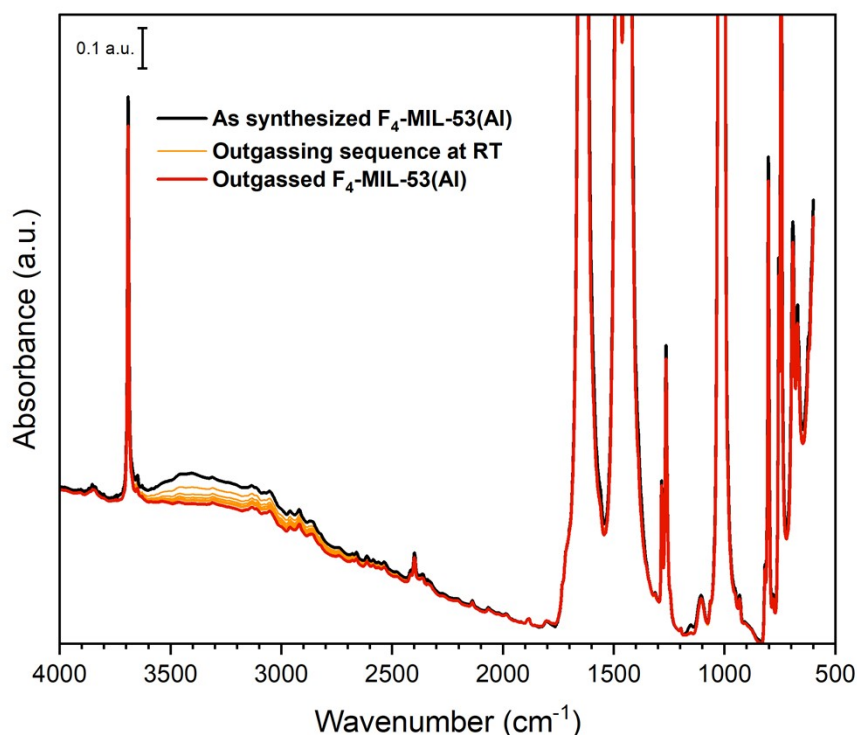


Figure S8. IR spectra of $F_4\text{-MIL-53(Al)}$ during outgassing at room temperature (RT).

The IR spectral profile of structural hydroxyl groups can also be an indication of the phase transition from narrow pore (np) to large pore (lp). Generally, the transition occurs with evacuation of the sample, namely by removing the water molecules present inside the pores and results in a slight shift towards higher frequencies of the ν_{OH} due to a modification in the extent of the H-bonding between hydroxyls and pore walls.⁷ Concerning $F_4\text{-MIL-53(Al)}$, the ν_{OH} band is not perturbed upon outgassing. This suggests that no phase transition ($lp \leftrightarrow np$) occurs, due to the very low uptake of water when the MOF is simply air exposed. The very sharp and isolated nature of the signal at 3692 cm^{-1} also suggests the presence of a single phase and excludes the coexistence of np and lp structures in the as synthesized sample.

VT-PXRD

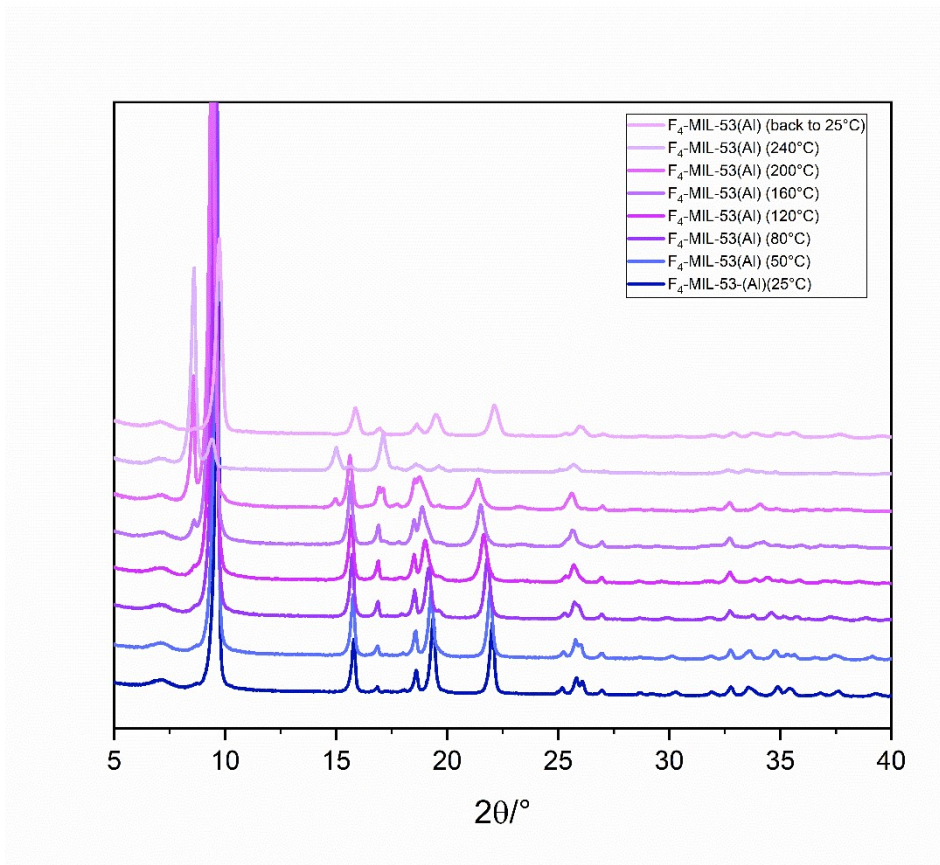


Figure S9. VT-PXRD patterns of F_4 -MIL-53(Al)

Table S2. Comparison between the lattice parameters of np and lp phase of F_4 -MIL-53(Al).

| | np phase | lp phase |
|-------------------------------|--------------|------------|
| Symmetry | Orthorhombic | Monoclinic |
| Space group | $Imma$ | $P2_1/c$ |
| a [Å] | 6.6295(13) | 12.43 (1) |
| b [Å] | 18.108(4) | 18.94(2) |
| c [Å] | 10.747(2) | 6.328(4) |
| β | -- | 84.56(10) |
| Volume [Å³] | 1292.1(8) | 1482(2) |

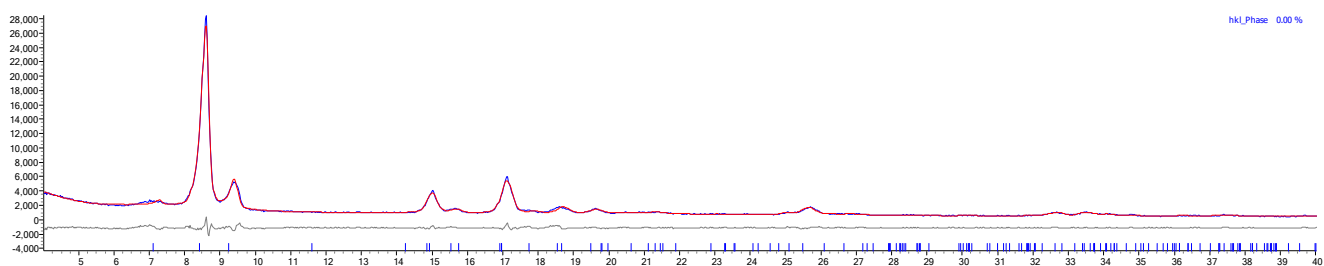


Figure S10. Pawley fit carried out on the PXRD pattern ($\lambda = 1.5401 \text{ \AA}$) of F_4 -MIL-53(Al) lp phase. The experimental PXRD pattern is shown in blue, the calculated in red and the difference (observed - calculated) is given in grey. The allowed reflection positions are given in blue. ($R_{wp} = 16.3706$, $R_p = 10.5080$)

Differential scanning microscopy (DSC)

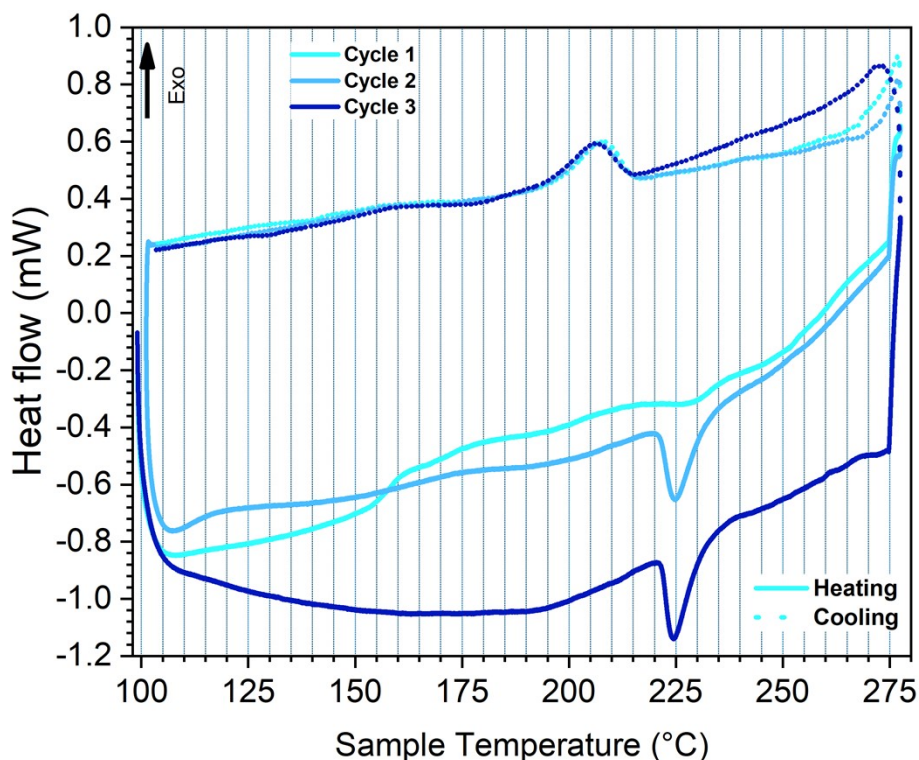


Figure S11. DSC profile of F4-MIL-53(Al) (right): first cycle (cyan), second cycle (light blue) and third cycle (blue). Full and dotted curves refer to the heating and cooling cycles respectively.

Bibliography

- 1 A. X. S. Bruker, *Bruker AXS, Karlsruhe, Germany*.
- 2 J. Laugier and B. Bochu, *Laboratoire des Matériaux et du Génie Physique de l'Ecole Nationale Supérieure de Physique de Grenoble (INPG), France*.
- 3 R. Černý and V. Favre-Nicolin, *Powder Diffr*, 2005, **20**, 359–365.
- 4 Y. Hu, X. Dong, J. Nan, W. Jin, X. Ren, N. Xu and Y. M. Lee, *Chemical Communications*, 2011, **47**, 737–739.
- 5 M. Mihaylov, K. Chakarova, S. Andonova, N. Drenchev, E. Ivanova, A. Sabetghadam, B. Seoane, J. Gascon, F. Kapteijn and K. Hadjiivanov, *Journal of Physical Chemistry C*, 2016, **120**, 23584–23595.
- 6 J. M. Salazar, G. Weber, J. M. Simon, I. Bezverkhyy and J. P. Bellat, *Journal of Chemical Physics*, DOI:10.1063/1.4914903.
- 7 C. Volkringer, T. Loiseau, N. Guillou, G. Férey, E. Elkaïm and A. Vimont, *Journal of the Chemical Society. Dalton Transactions*, 2009, 2241–2249.
- 8 K. I. Hadjiivanov, D. A. Panayotov, M. Y. Mihaylov, E. Z. Ivanova, K. K. Chakarova, S. M. Andonova and N. L. Drenchev, *Chem Rev*, 2021, **121**, 1286–1424.

